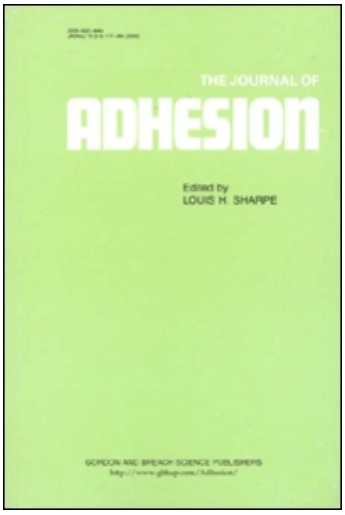

The Journal of Adhesion
Publication details, including instructions for authors and subscription information:
http://www.informaworld.com/smpp/title~content=t713453635

Characterized Metal Microcontacts

J. B. Pethica[ab]; D. Tabor[a]
[a] Cavendish Laboratory, University of Cambridge, Physics and Chemistry of Solids, Cambridge, England [b] Brown Boveri Forschungszentrum, Switzerland

To cite this Article Pethica, J. B. and Tabor, D.(1982) 'Characterized Metal Microcontacts', The Journal of Adhesion, 13: 3, 215 — 228
To link to this Article: DOI: 10.1080/00218468208073188
URL: http://dx.doi.org/10.1080/00218468208073188

J. Adhesion, 1982, Vol. 13, pp. 215–228
0021–8464/82/1304–0215 $06.50/0

Printed in Great Britain

Characterized Metal Microcontacts

J. B. PETHICA† and D. TABOR

University of Cambridge, Physics and Chemistry of Solids, Cavendish Laboratory, Madingley Road, Cambridge CB3 0HE, England

(*Received June 9, 1981: in final form August 11, 1981*)

This paper describes a study of the contact between a fine tungsten point and a flat single crystal of nickel over a load range of approximately 1 to 1000 μN. The experiments are carried out in an ultrahigh vacuum (10^{-10} torr) scanning electron microscope with an Auger facility for characterising the nickel surface *in situ*. Electrical resistance measurements provide a reasonable estimate of the area of contact both on loading and unloading. The results show that even for zero joining load finite adhesion is observed, the unloading involving plastic deformation. A partial monolayer of oxygen has no effect on the adhesion: one or two monolayers produce some reduction: an oxide film about 5 nm thick produces a marked reduction in adhesion until, at a critical load, the oxide is penetrated. The results are discussed in terms of surface energy, ductility and fracture mechanics.

INTRODUCTION

The cohesive atomic forces within bodies act for some distance beyond their boundaries. An energy $\Delta\gamma$ per unit area is thus released when two bodies are brought into contact. The mechanical effects of this surface energy are easily evaluated in liquids. However, in solids, energy may be stored or expended in elastic or plastic deformation processes. Thus to calculate the adhesive effects of surface forces, one needs to know the contacting geometry and the mode of deformation. The simplest geometry to consider is that of contacting spheres. Other, complex surfaces can often be modelled as combinations of spheres of various radii. In what follows we shall deal only with the contact between a sphere of radius R and a flat surface.

There are two extreme ways in which the interaction may occur.

If the spheres are perfectly elastic Derjaguin, Muller and Toporov[1] (DMT) suggested that the deformation would follow the classical laws of Hertz[2] and that an appreciable contribution to the interaction would result from surface

† Present address: Brown Boveri Forschungszentrum, Dättwil CH-5405, Switzerland.

forces outside the immediate zone of contact. By contrast Johnson, Kendall and Roberts[3] (JKR) showed that the Hertzian stress field must be modified by the surface forces: for deformable solids a neck is formed around the region of contact and all the interaction is assumed to be restricted to the contact zone itself. More recently Muller *et al.*[4] have shown that the JKR solution merges into the DMT solution as the height of the neck becomes smaller than the effective range of the surface forces. Thus the JKR model holds better for materials of low modulus and/or short range surface forces. Their treatment gives a value for the adhesive force of $3/2\ \pi R\Delta\gamma$ whereas the DMT model gives an adhesive force of $2\pi R\Delta\gamma$. It is evident that the actual magnitude of the adhesive force does not differ greatly in the two models. Further, if the surfaces are not smooth high asperities will tend to prise the surfaces apart thus reducing the observed adhesion.[9] This will be more marked for bodies of high elastic modulus.

In the experiments described in this paper the size of the sphere and the modulus of the surfaces are such that the elastic behaviour is closer to the JKR model. Our discussion will therefore refer primarily to this model and the way in which this model may itself be modified by the occurrence of plastic deformation.

In contacts involving largely plastic deformation, the energy expended in plastic flow is usually much greater than the surface energy in the contact. Surface forces may therefore often be disregarded if the loading is sufficient to produce appreciable plastic flow. The deformation is then described in terms of the indentation hardness H, the mean pressure between the surfaces when the deformation is fully plastic.[6] When the joining load is removed, stored elastic stresses are released. For contacting spheres, the value of R in the contact zone will increase.[6] Johnson[7] has shown that the force of adhesion is then given by $E^*\Delta\gamma D/H$ where D is the diameter of the indentation previously made and $E^* = ((1-v_1^2)/E_1 + (1-v_2^2)/E_2)^{-1}$, v and E being Poissons ratio and Youngs modulus respectively of spheres 1 and 2. If $H < (4E^*\Delta\gamma/\pi D)^{1/2}$ then the mean interfacial pressure will exceed H, and separation may be expected to involve fully plastic flow at a stress equal to H. This is similar to the tensile extension of a deeply notched bar.[8] The adhesive force is equal to the original joining load.

The major difficulties in applying these ideas are that there is little reliable data for $\Delta\gamma$ and that for very small contact regions H may be considerably different from the bulk value[9] and may be influenced by the surface.[10]

The work described here is aimed at clarifying some of the above processes. To be certain that the surfaces under investigation are free from contaminants, experiments are performed in an ultra-high vacuum system with *in situ* surface cleaning and Auger analysis facilities. To avoid macroscopic roughness, the contacting geometry is that of a very sharp point ($R \sim 2\ \mu$m) contacting a flat

single crystal face. This also allows the study of microhardness phenomena. Such a geometry was used by Pollock *et al.* in a study similar to the one described in this paper but these workers were unable to characterise their surfaces *in situ*. By contrast Buckley[12] carried out elegant experiments in UHV on well characterised surfaces but they were nominally flat so that the nature of the contact was uncertain. In the present experiments the contacting processes are observed by an *in situ* scanning electron microscope (SEM) and, because of the very small contacting forces involved, the whole apparatus is carefully isolated from possible sources of vibration.

EXPERIMENTAL

The experiments were performed in a Vacuum Generators Ltd. HB200 UHV scanning microscope. This uses a field emission source and very simple lens system to achieve an optimum resolution of about 400 Å. The specimen chamber is separately pumped by ion and titanium sublimation pumps, easily achieving a base pressure of 20 nPa. A trapped diffusion pump gave rapid removal of inert gases, but was not used during contact experiments due to its attendant vibrations. A set of retarding field electron energy analysing grids was installed for Auger analysis (AES), giving surface characterisation sensitive to 1% monolayer (ML).[13] Other facilities on the specimen chamber were an argon ion gun for sputter cleaning, a mass spectrometer, an auxiliary electron gun and optical viewpoints.

The mechanical arrangement of sharp point and flat is shown in Figure 1. Forces were generated electrostatically at one end of the arm and transmitted

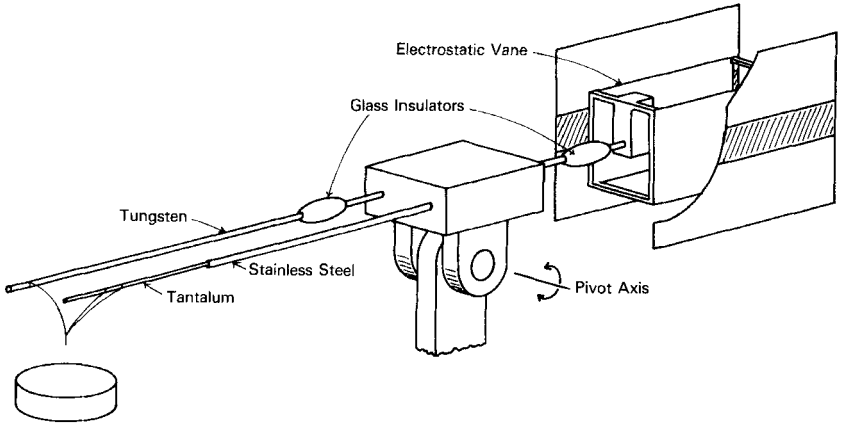

FIGURE 1 The loading arm (schematic).

via a spring pivot to the stylus at the other end. Up to 4 mN could thereby be applied to the tip. The advantages of a spring pivot over systems with sliding or rolling bearings include no starting friction to give erroneous loads, no problems of seizure in UHV, and easy, reliable electrical contact with the tip. The spring rate of the arm was first determined using weights, and then being known was used to calibrate the electrostatic loading system just prior to an experiment, using the SEM to measure deflection for a given voltage. The electrical resistance between point and flat was continuously monitored by a four terminal AC system. Initially this was a Keithley model 503 milliohm-meter, which dissipated powers of the order of 1 μW in the contact. Later, a more advanced system dissipating smaller powers and with a wider dynamic range was used.[14]

If the surfaces are clean, the contact diameter D may be deduced from the contact resistance r using the equation[15]

$$r = (\rho_1 + \rho_2)/2D$$

where ρ_1 and ρ_2 are the resistivities of the contacting materials.

The whole apparatus was mounted on air-filled tyres, and electrical and other connections made by long flexible leads. All experiments were performed in the early hours of the morning when the laboratory building was completely silent. These precautions allowed forces around 1 μN to be reliably measured. Further experimental details will be found elsewhere.[16]

Specimen preparation

The tungsten contacting stylus was formed by the same method as that used to make field emission tips, the etching in KOH being carried on somewhat longer to produce blunter points around 1–2 μm radius of curvature. The opposing flat surface was a single crystal (111) face of nickel in most of the experiments described here. (A gold single crystal was also used.) This was cut by spark machining after X-ray alignment, and then mechanically polished to $\frac{1}{4}$ μm. The crystal was then either electropolished or given a final mechanical polish with γ-alumina. No significant differences were observed in the results of subsequent experiments between these two final polishes.

Once installed in ultra-high vacuum, the specimen underwent fairly standard surface cleaning of repeated cycles of argon ion bombardment (400 V, 1μA/cm^2) followed by annealing (1000 K, up to two days) to remove bombardment damage.

Ten or more cycles were required to eliminate surface segregation of impurities, particularly of sulphur. Eventually, Auger analysis indicated an impurity (carbon) coverage of ca.0.07 ML. The tungsten tip was generally cleaned by heating to 2000°C. The Auger system could only analyse the whole

tip wire. Carbon contamination thus detected could be removed by flashing the tip in a few mPa of oxygen.

Contacts were made using the following procedure. The tip was positioned a few microns above a desired part of the surface using micrometer controls. The electrostatic loading voltage was then steadily increased, allowing the surfaces to approach, typically at 1 $\mu m/min$. The moment of contact was detected by a fall to a finite value of the contact resistance; it could also, if required, be estimated knowing the deflection of the arm for a given loading voltage. The load was then increased steadily to the desired value. Pull-off was accomplished by reversing the direction of the loading voltage ramp. The moment of separation was also indicated by contact resistance, and if adhesion was appreciable, by an obvious sudden jump up of the arm. Load voltage and contact resistance were continually monitored during the above procedure.

Results

In an individual contact, a maximum joining load P_0 is applied; from hence the load is decreased till separation occurs. The value of negative load Z to produce separation is plotted against P_0 in Figure 2. The important features

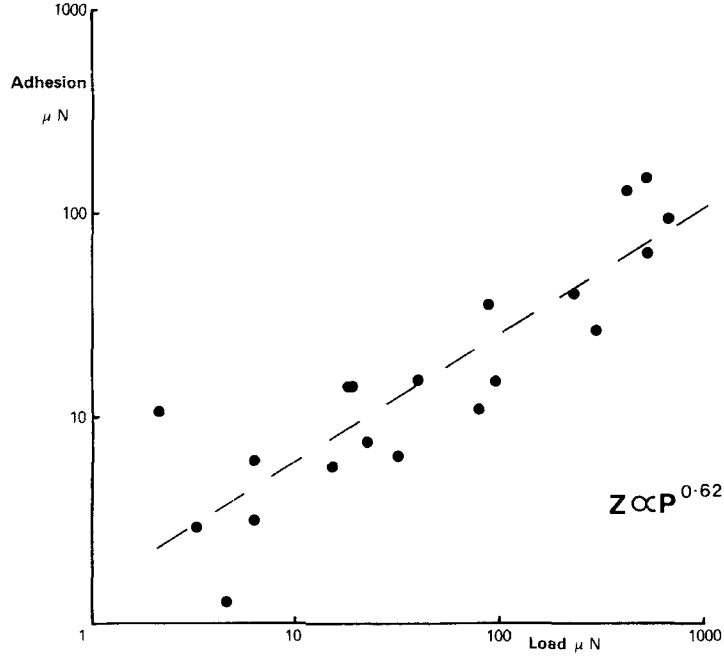

FIGURE 2 Adhesion of tungsten tip to a clean nickel surface expressed as adhesive force Z *v.* the joining load P.

are that adhesion generally increases with load and is small at low loads. Unlike Gane, Pfaelzer and Tabor[17] and Maugis *et al.*,[18] adhesions greater than the applied load were properly observed only once or twice. Simultaneous viewing with the SEM showed that many such measurements were due to an obvious external vibrational impulse; as a result these obvious cases were not used here.

If the surfaces are perfectly clean, if there is no vibration and roughness effects are absent the adhesion for elastic deformation should be constant at a value of $3\pi R\Delta\gamma/2$; *i.e.*, for $R = 2$ μm and $\Delta\gamma = 1$ Jm^{-2}, adhesion should be 10 μN. Our data at very low applied loads show considerable scatter with adhesions between 1 and 10 μN. In view of the precautions taken to avoid vibrations this scatter may be due to the random encounter of small patches of contaminant of the flat surface. The Auger beam covers an area of 1 mm^2 and thus cannot detect such patches.

It is seen from Figure 3 that the overall resistance trace is irreversible: the contact diameter D remains almost constant on unloading till just before separation. This implies ductile failure of the junction. From Figure 4 it is seen that the adhesion force Z is nearly proportional to D^2 and thus that the separating stress is roughly constant, with a typical value of 1.4 GPa. This is about twice the macroscopic indentation hardness of nickel, the weaker metal in the contact. The indentation hardness may also be estimated from Figure 5. The mean value is approximately 2.4 GPa, between three and four times the bulk hardness of nickel.

We also note that ductile separation implies some material transfer as a result of contact. Unfortunately the electron beam used in the Auger facility is relatively wide and this makes it impossible to detect such transfer. A fine "spot" Auger system, now under construction, should resolve this difficulty.

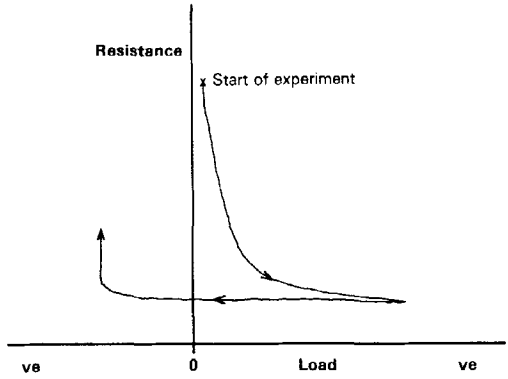

FIGURE 3 Typical result for clean surfaces showing the variation of contact resistance as contact is made (positive load) and broken (negative load).

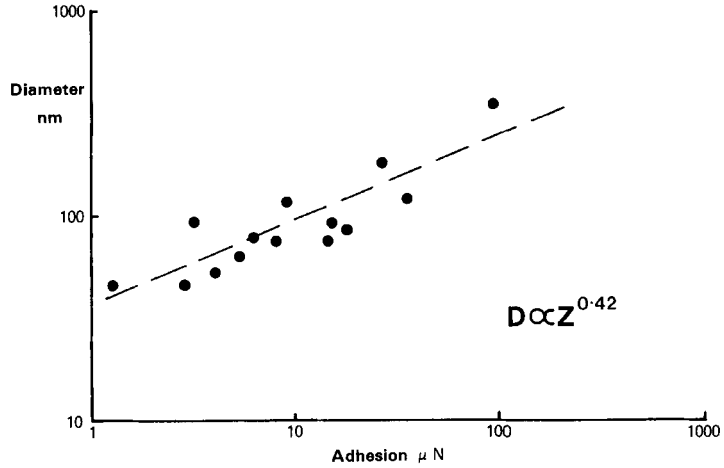

FIGURE 4 Contact of clean surfaces. The adhesion force Z is plotted as a function of the diameter D of the circle of contact. D is deduced from the electrical contact resistance. Z is approximately proportional to the area of contact (D^2) implying that the separating stress is roughly constant.

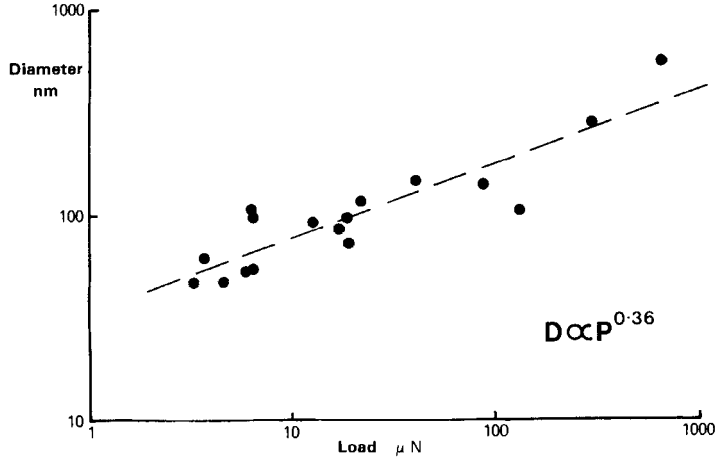

FIGURE 5 Contact of clean surfaces. The diameter D of the circle of contact is plotted as a function of the joining load P. D is deduced from the electrical contact resistance.

Oxidised surfaces

The nickel surface was lightly oxidised by simply admitting oxygen gas to the specimen chamber with controlled pressure and time of exposure. The oxidation state of the surface was judged by comparison with comparable exposures in the work of Holloway and Hudson[19] and Ahmad.[20] The

tungsten was normally cleaned by flashing to 2000°C which removes the oxygen as the volatile WO_3.

Oxygen exposures of 3 mPa.sec. which produce less than a monolayer coverage did not give rise to any significantly different contact behaviour from that described previously for clean surfaces. Exposures of up to 0.15 Pa.sec. which should give one to two monolayers coverage, resulted in an overall increase in contact resistance of a factor of four or so, accompanied by a rise in resistance towards the end of unloading. This latter suggests that the unloading process is becoming more elastic. The overall rise in resistance is no longer solely due to current constriction, and since the film resistivity is unknown, absolute values of diameter are not obtainable.

To generate thicker oxide films, the nickel was heated to 300°C and exposed to about 10 Pa.sec. of oxygen. This should give an oxide film on the nickel surface of approximately 5 nm thickness.[20] The behaviour of contact resistance under these conditions is depicted in Figure 6. Upon initial contact the resistance was extremely high. This made it difficult to judge the moment of contact and hence Z and P_0 to an accuracy greater than $\sim 2\,\mu$N. The resistance was also fairly reversible upon unloading. However, above a critical load of

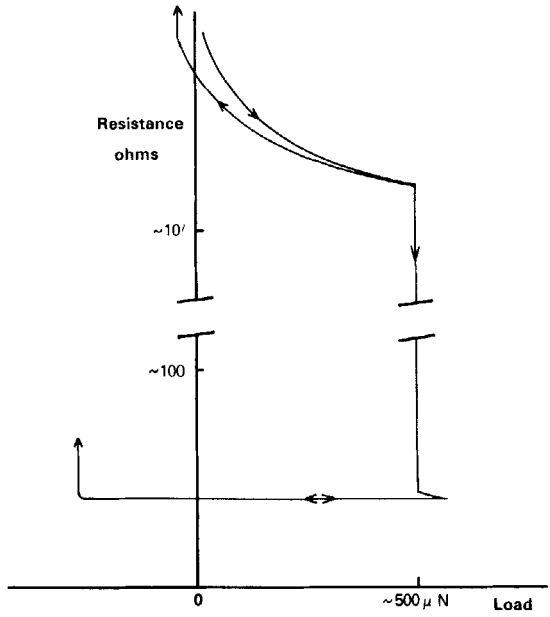

FIGURE 6 Contact between a clean tungsten tip and a nickel surface covered with a layer of oxide a few nm thick. Electrical contact resistance as a function of load. For loads less than about 500 μN the resistance is very high and the contact behaviour almost reversible. Above this load the oxide is penetrated and the resistance behaviour resembles that of clean metals.

700 ± 200 μN, the resistance suddenly fell by several orders of magnitude and subsequently showed an approximately constant value upon unloading. This implies that the oxide film has been penetrated and that the subsequent behaviour is similar to that of clean metals in contact. The variation of adhesive force Z with load P_0 (Figure 7) supports this idea, the adhesion of penetrated films approaching that of clean surfaces.

If we assume Hertzian elastic loading conditions prior to penetration, as implied by reversible contact resistance, we have

$$D^3 = 6RP_0/E^*$$

This assumes that the whole of the elastic stress is supported by the metallic substrate and that the oxide film provides negligible elastic stiffening. Using $R = 2$ μm (SEM observation), $P_0 = 0.9$ mN (maximum value from Figure 7) and $E^* = 140$ GPa (the effective bulk modulus for a W–Ni contact) we obtain a value $D \sim 43$ nm. This may be compared with the oxide film thickness *ca.* 5 nm. Thus the diameter of the circle of elastic contact is about nine times the film thickness. If the oxide provides additional stiffening the value of D will be smaller. Using the calculated value of D we obtain a maximum contact pressure prior to penetration of 6 GPa. If this corresponds to the onset of subsurface plastic deformation (Hertzian model) this implies a maximum shear stress under the contact of about 3 GPa. This is approximately $G/30$ where G is the shear modulus of nickel. This is in the region expected for the theoretical lattice strength.[21] In the absence of direct measurements of hardness just after film penetration (due to poor SEM resolution) it is reasonable to assume that the hardness is similar to values obtained from clean surfaces, since the adhesions after the penetration are similar to those of clean surfaces.

Gane,[9] working with poorly characterised surfaces, found sudden penetration at a critical load, with no deformation visible beforehand. He suspected that a surface film of polymer (generated from organic vapours present in the chamber of his microscope) may have been present, since very carefully prepared surfaces did not show sudden penetration. He estimated strengths prior to penetration assuming that the contact was elastic. His results parallel those obtained here, and we may compare the estimates of strength. In the period before penetration shear strains of over 3% were observed here compared with up to 5% observed by Gane. After sudden indentation Gane observed hardness values in gold of 0.7–0.8 GPa, two to three times the bulk value. Here hardnesses ranging from two to four times the bulk value of nickel were observed for clean and post-penetration surfaces. The results presented here can be seen to tie in with those of Gane.[9]

The behaviour prior to oxide penetration may not be entirely elastic, since Z varies somewhat with P_0 (Figure 7), so that the values of contact pressure in

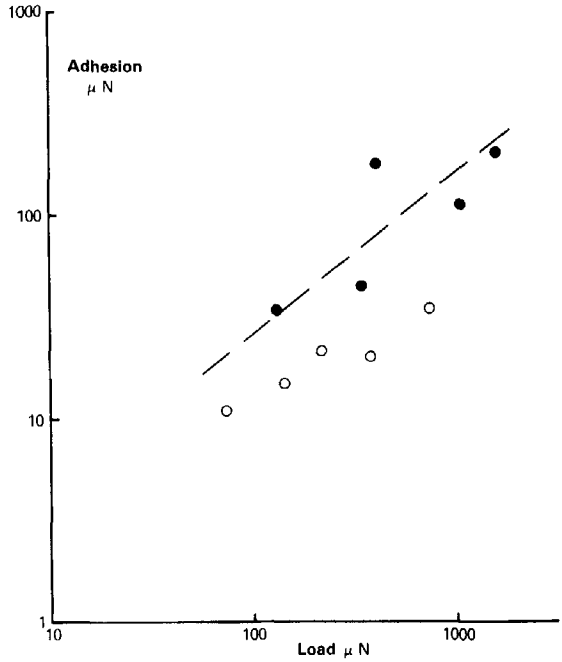

FIGURE 7 Adhesion versus load in the presence of an oxide film: ○ before oxide penetration: ● after oxide penetration: — — — typical clean surface behaviour.

the present and Gane's work would be overestimated. However, plastic deformation is probably small, since Gane could not see any pre-penetration deformation in his experiments. Again, in the present experiments the contact resistance is largely reversible till penetration.

Finally, it was noted that the resistance of the thin oxide film prior to penetration was non-ohmic, falling by a factor of three as the applied voltage rose from 0.3 to 1 volt.

DISCUSSION

In the clean tungsten-nickel contacts described above, the loading process at loads around 5–10 μN may be elastic. However, even at the smallest loads the unloading behaviour seems to involve plastic, ductile extension of the contact junction. Therefore, surface forces are strong enough to prevent reversible separation along the original interface. At higher loads, the indentation process undoubtedly involves plastic deformation. Under these conditions, as mentioned earlier, Johnson[7] has shown that ductile separation should occur

provided

$$H^2 < 4E^*\Delta\gamma/\pi D \tag{1}$$

Using $D = 10^{-7}$ m, $\Delta\gamma = 2\,\mathrm{J/m^2}$ and $E^* = 140$ GPa we find that for ductile separation H should be less than 1.8 GPa. This may be compared with $H = 1.5$ to 2.4 GPa derived from our contact resistance measurements for clean contacts. Thus the criterion for ductile separation is close to being satisfied. This conclusion should be contrasted with the behaviour in the presence of an oxide film where H rises to values of the order of 4 to 6 GPa. In this case the above criterion will no longer hold and separation should occur at the original interface in a brittle, elastic manner. This is indeed observed prior to penetration of the oxide film. When penetration has occurred, the hardness falls and both the adhesion and resistance behaviour are similar to those of a clean surface. We recall here the formula due to Johnson[7] for brittle separation following a plastic indentation

$$Z = 2E^*\Delta\gamma(P_0/\pi H^3)^{1/2} \tag{2}$$

The variation of adhesion Z with hardness H is plotted in Figure 8. For plastic separation [Eq. (1) satisfied] $Z = P_0$. For brittle separation, which will occur for high H values, the adhesion falls with increasing H. The mode of separation and adhesive force may thus be seen to depend on H.

Further, as can be seen from Eq. (1), a decrease in $\Delta\gamma$ could also give a transition to brittle separation and reduction in adhesion; it is not as sensitive a parameter as H. For organic adsorbates, where bonding could be reduced to van der Waals, a significant drop in $\Delta\gamma$ could occur and is the commonly given

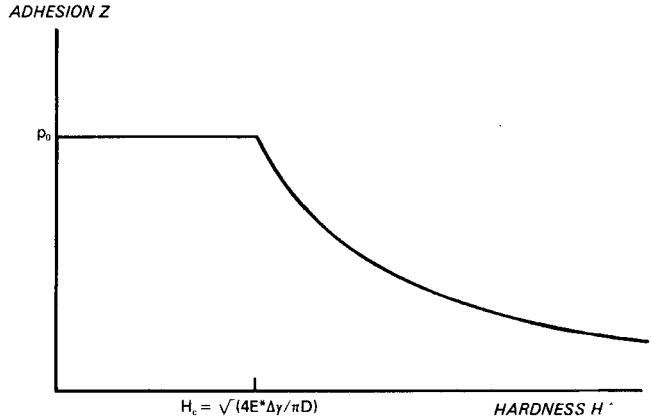

FIGURE 8 Theoretical curve showing variation of adhesion Z with hardness H for constant P_0, E^* and $\Delta\gamma$. For low hardness values the separation is ductile and the adhesion Z is equal to the joining load P_0. Above a critical value of the hardness [see Eq. (1)] separation is brittle and the adhesion falls off with increasing hardness [see Eq. (2)].

reason for the low adhesion of grossly contaminated metals. Work by Hondros[22] suggests that $\Delta\gamma$ falls even for monolayer coverages of oxygen. In the work of Hondros and McLean[23] the decrease in $\Delta\gamma$ caused by grain boundary segregation of Bi in Cu is proposed as the main reason for the attendant grain boundary embrittlement. This has been disputed by Seah.[24] In the present work, no direct measurements of $\Delta\gamma$ could be made; consequently its relative importance cannot be judged, but it is clear that an increase in H occurs and can easily be a major cause of loss of ductility in the contact.

We have so far considered the unloading and separating process. We now consider the loading process; for loads much greater than 10 μN it is generally plastic for clean surfaces. At lower loads the variation of diameter with loads suggests Hertzian (elastic) behaviour. However, this does not account for the action of surface forces. According to the JKR model, surface forces should give a constant adhesive force around 10 μN for the lowest joining loads. The data of Figure 2, however, shows a rather large scatter. As we have previously noted, this might be due to patches of contaminant giving local variations in $\Delta\gamma$. The large scatter may also be due to surface roughness.[5,7] On the scale of the present experiments these roughnesses would correspond to surface steps of as little as two or three atoms height. We consider here their effect on the loading process.

The edge of the contact zone may be regarded as a crack resealing under the influence of surface forces. The range of these forces in metal bonding is extremely short, of about 0.2 or 0.3 nm,[25] falling very rapidly beyond this range. When, in the approach to JKR equilibrium on initial contact, the crack reaches a step of height greater than this range (Figure 9), that is, two to three atoms in height, its progress may be halted. This means that the contact area and hence the adhesion will be smaller than predicted by JKR. This view of action of surface forces is rather different from the contact models cited above, which use hemispherical asperities with a range of radii of curvature to

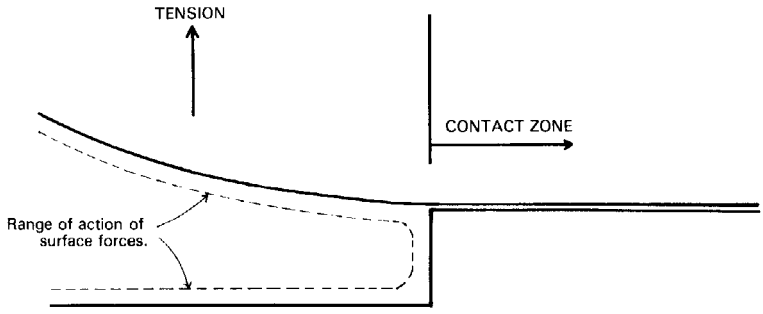

FIGURE 9 Crack tip consisting of a step a few atoms in height (schematic).

simulate surface roughness. We have not considered here the possibility that surface forces may actually generate plastic deformation.

Finally we consider the magnitude of the indentation hardness. With clean surfaces the hardness is higher than the bulk hardness but only by a factor of 2 or 3. By contrast very high values are observed in the presence of a surface film. Why this is so is not clear. It may be due to the elastic mismatch of film and substrate trapping or impeding dislocations. The subject of surface hardening (or softening) is under much dispute, and many theories are advocated without any clear experimental consensus.[10] We may also ask the inverse question, that is, why such small stressed volumes as those of the present work do not show theoretical lattice strength when clean. It is possible that surface steps and facets act as stress concentrators and facilitate dislocation punching, for example, of loops, as discussed by Gane[9] and Brown and Woolhouse.[26] This punching and subsequent propagation might be impeded by surface films, allowing the exhibition of hardnesses similar to those expected from a theoretically perfect lattice.

CONCLUSIONS

For the tungsten nickel microcontacts studied in this paper the mechanism of separation when the surfaces are clean, involves plastic deformation. The hardness of the clean nickel surface is a factor of two or three above the macroscopic value, but still some way below that expected from the perfect lattice. The presence of an oxide film of about 5 nm thickness increases the hardness and, below a critical load causes the contact separation process to become brittle. The oxide film can be penetrated by a sufficiently large load, hence giving rise to metallic contact and plastic behaviour.

References

1. B. V. Derjaguin, V. M. Muller and Yu. P. Toporov, *Journal of Colloid & Interface Science* **53,** 314–326 (1975).
2. H. Hertz, *Miscellaneous Papers* (Macmillan, London, 1896), p. 146.
3. K. L. Johnson, K. Kendall and A. D. Roberts, *Proc. R. Soc. Lond.* **A324,** 301–313 (1971).
4. V. M. Muller, V. S. Yushchenko and B. V. Derjaguin, *Journal of Colloid & Interface Science* **77,** 91–101 (1980).
5. K. N. G. Fuller and D. Tabor, *Proc. R. Soc. Lond.* **A345,** 327–342 (1975).
6. D. Tabor, *The Hardness of Metals* (Clarendon Press, Oxford, 1951).
7. K. L. Johnson, *Theoretical and Applied Mechanics*, W. T. Koiter, Ed. (North Holland, Delft, 1976), p. 133.
8. E. Orowan, *Rept. Prog. Phys.* **12,** 185–232 (1949).
9. N. Gane, *Proc. R. Soc. Lond.* **A317,** 367–391 (1970).
10. R. M. Latanision and J. T. Fourie, *Surface Effects in Crystal Plasticity* (Noordhoff, Leyden, 1977).
11. H. M. Pollock, P. Shufflebottom and J. Skinner, *J. Phys. D; App. Phys.* **10,** 127–138 (1977).

12. D. Buckley, NASA Report 5756 (1970); NASA Report TND 5922 (1970); *Wear* **20,** 89–103 (1972); NASA Report TND 7896 (1975).
13. C. C. Chang, in *Characterization of Solid Surfaces*, Kane and Larrabee, Eds. (Plenum Press, New York, 1974), Chap. 20.
14. M. D. Pashley and J. B. Pethica, *J. Phys. E; Sci. Inst.* **14,** 584–586 (1981).
15. R. Holm, *Electric Contacts Handbook* (Springer-Verlag, Berlin, 1967).
16. J. B. Pethica, Ph.D. Thesis, University of Cambridge (1978).
17. N. Gane, P. F. Pfaelzer and D. Tabor, *Proc. R. Soc. Lond.* **A340,** 495–517 (1974).
18. D. Maugis *et al.*, *ASLE Transactions* **21,** 1–19 (1976).
19. P. H. Holloway and J. B. Hudson, *Surf. Sci.* **43,** 141–149 (1974).
20. K. Ahmed, Ph.D. Thesis, University of Cambridge (1977).
21. A. Kelly, *Strong Solids* (Clarendon Press, Oxford, 1973).
22. E. D. Hondros, *Acta Met.* **16,** 1377–1380 (1968).
23. E. D. Hondros and D. McLean, D., *Phil. Mag.* **29,** 771–795 (1974).
24. M. P. Seah, *Surf. Sci.* **53,** 168–212 (1975).
25. J. E. Inglesfield, *J. Phys. F.; Met. Phys.* **6,** 687–701 (1976).
26. L. M. Brown and G. R. Woolhouse, *Phil. Mag.* **21,** 329–345 (1970).